



Electronic properties of single semiconductor nanocrystals: optical and electrostatic force microscopy measurements

Todd D. Krauss *, Louis E. Brus

Department of Chemistry, Columbia University, 2960 Broadway, New York, NY 10027, USA

Abstract

We review the room temperature optical and electronic properties of single semiconductor nanocrystals, which are made by chemical synthesis. Confocal luminescence spectroscopy of single nanocrystals reveals a blinking behavior apparently due to an intermittent photoionization. To investigate this further, the dielectric constant and electrostatic charge of single CdSe nanocrystals was measured. The static dielectric constant among single CdSe nanocrystals is uniform, and its value is consistent with the value of the dielectric constant of the bulk material. However, the electrostatic polarization among individual nanocrystals is non-uniform, with a significant fraction of the nanocrystals possessing a partial positive charge ($Q \sim 0.5 e$), and/or a permanent dipole ($P \sim 35 D$). A small fraction of the nanocrystals has a positive polarization, which blinks 'on' and 'off' over time. In addition, photoexcitation with frequencies greater than the band gap of the nanocrystal results in photoionization. © 2000 Elsevier Science S.A. All rights reserved.

Keywords: Semiconductor; Nanocrystal; Single; Electronic

1. Introduction

Semiconductor nanocrystals have attracted much attention over the last decade due to their unique physical properties, and potential use for a wide range of applications ranging from all optical switching to biological labels (for a recent review, see Refs. [1,2]). While the optical, electronic and vibrational properties of semiconductor nanocrystals have been studied extensively, the electrostatic properties have received little attention. Understanding the electrostatic properties of single semiconductor nanocrystals is of fundamental interest. Furthermore, the electrostatic properties of a nanocrystal significantly affect its optical, electronic, and vibrational characteristics, thus necessitating further investigation. In addition, the blinking, or on–off behavior, recently observed in single-CdSe nanocrystal photoluminescence [3] is tentatively attributed to an intermittent photoionization and subsequent neutralization of the nanocrystal. Thus, measurements of the electrostatic properties of individual nanocrystals can elucidate the physical mechanisms underlying this interesting photoluminescence behavior.

Although electronically different from the bulk material, a nanocrystal has a crystal lattice identical to the bulk material. Bulk CdSe crystallizes in the wurtzite structure, which contains a structural dipole moment along the c -axis. Thus, in the simplest picture, CdSe nanocrystals should contain a permanent electrostatic polarization. Also, the magnitude of this polarization should increase with the volume of the nanocrystal. However, recent theoretical treatments have predicted the absence of a correlation between dipole moment and nanocrystal size [4]. In addition, the important effect of screening of any structural dipole moment has not yet been investigated.

Prior investigations have only indirectly measured, or only inferred, the presence of a permanent electrostatic polarization of semiconductor nanocrystals. Screened dipole moments, which scaled in magnitude with nanocrystal size, were determined from dielectric dispersion measurements of ensembles of CdSe nanocrystals [5]. Ensemble measurements of exciton–phonon coupling [6], two-photon fluorescence excitation [7], and Raman depolarization [8], suggest a permanent electrostatic polarization in the nanocrystal as well. Finally, quantum-confined Stark measurements of single nanocrystals [9] also imply the presence of permanent electric fields in the nanocrystal.

* Corresponding author. Tel.: +1-212-854-3553; fax: +1-212-932-1289.

E-mail address: krauss@chem.columbia.edu (T.D. Krauss)

2. Confocal luminescence

Nanocrystals are extremely interesting and useful in part, because their optical, vibrational, and electronic properties depend strongly on size [10–12]. However, since even the highest quality samples contain inhomogeneities in size, shape and surface chemistry, this practical benefit can obscure physical phenomena under study. This motivated recent single nanocrystal photoluminescence studies, which have revealed new physical processes such as fluorescence intermittency [3], and spectral diffusion [9,13] (for a review of single nanocrystal luminescence, see Refs. [14,15]).

The fluorescence intensity of a single CdSe nanocrystal over time is shown in Fig. 1. In contrast to previous ensemble measurements, the luminescence turns on and off ('blinks') on a several second time scale. Luminescence intensity measurements taken as a function of excitation intensity show that the 'on' periods scale inversely with laser intensity, while the 'off' periods are independent of laser intensity [3]. Furthermore, overcoating the nanocrystal with several monolayers of ZnS significantly increased both the on and off times. In fact, the on and off times were found to monotonically increase with increasing ZnS shell thickness. Together, these results suggest that a non-emissive state is created via photoexcitation of the nanocrystal.

A mechanism consistent with the observed blinking behavior in single nanocrystal photoluminescence involves Auger photoionization [3,16]. At excitation intensities typical of these experiments, there exists a small, but not insignificant, probability that two electron-hole pairs will be simultaneously excited. Annihilation of one electron-hole pair may result in a transfer of energy to the remaining carriers, one of which can then be ejected from the nanocrystal. Photoexcitation of the resulting ionized nanocrystal leads to Auger non-radiative decay, with little emission quantum yield [17]. Eventually, the nanocrystal is neutralized by the return of the ejected carrier, and the emission is restored. This proposal can be confirmed by experiments, which correlate luminescence blinking with photoionization of the

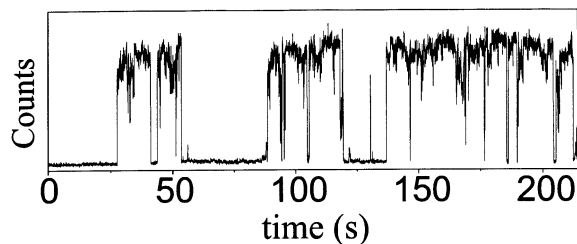


Fig. 1. Fluorescence intensity versus time trace of a single CdSe nanocrystal, adapted from Ref. [3]. The excitation intensity is $\sim 0.5 \text{ kW cm}^{-2}$, the excitation wavelength $\lambda = 532 \text{ nm}$, and the time between consecutive samples is 40 ms.

nanocrystal, thus motivating measurements of electrostatic properties of individual nanocrystals.

3. Electrostatic force microscopy (EFM)

3.1. Method

If a conductive atomic force microscope (AFM) tip is electrically connected to a conductive substrate, they will form a capacitor with capacitance C . The application of a variable dc voltage V_{dc} , and an ac voltage, $V_{\text{ac}} \sin(\omega t)$, to the tip results in an electrostatic attraction between the tip and the substrate. In addition, localized, static charge on the sample surface Q will interact with any charge on the tip (including induced charge due to Q , Q_{ind}), to produce additional forces on the AFM tip. Approximating these surface charges as point charges, the force on the tip is given by [18,19]:

$$F_{\text{dc}} = \frac{Q(Q_{\text{ind}} + CV_{\text{dc}})}{4\pi\epsilon_0 z^2} + \frac{\partial C}{\partial Z} \left(\frac{V_{\text{dc}}^2 + \frac{V_{\text{ac}}^2}{2}}{2} \right) \quad (1)$$

$$F(\omega) = \left(\frac{\partial C}{\partial Z} V_{\text{dc}} + \frac{QC}{4\pi\epsilon_0 z^2} \right) V_{\text{ac}} \quad (2)$$

$$F(2\omega) = \frac{\partial C}{\partial Z} \frac{V_{\text{ac}}^2}{4} \quad (3)$$

where $F(\omega)$ and $F(2\omega)$ are the components of the force at the ac voltage frequency ω and 2ω , respectively, ϵ_0 is the static dielectric constant, and z is the distance between the tip and the conductive substrate. With the aid of lock-in amplification, the magnitude of local surface charge (Q) can be easily determined from the force on the tip at ω . Furthermore, for an insulating sample, local dielectric properties can be determined from the component of the force at 2ω , through $\partial C/\partial z$.

The basic experimental procedure for EFM consists of measuring the effect of electrostatic forces on the AFM tip while it is vibrating above a sample surface. For small vibrational amplitudes, the electrostatic force on the tip is approximated as a simple-harmonic type interaction [20]. Thus, the electrostatic force gradient normal to the surface, F' , acts as an effective spring constant, which slightly shifts the resonance frequency of the cantilever. Assuming that F' does not significantly affect the vibration of the cantilever, the shifted resonance frequency is given by:

$$\Delta\nu \approx -\frac{\nu}{2k} \frac{\partial F}{\partial z} \quad (4)$$

where ν is the cantilever resonance frequency, and k is the cantilever spring constant. The negative sign arises because an increasingly attractive force decreases the cantilever resonance frequency [20]. This simple technique effectively decouples electrostatic forces from

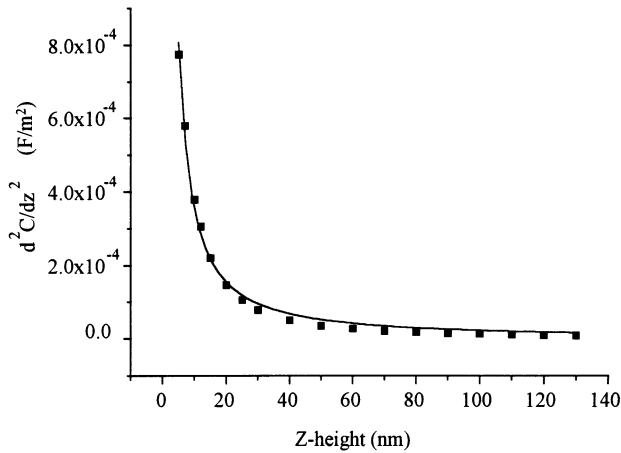


Fig. 2. d^2C/dz^2 versus z . The squares are the experimental data and the solid line is a power-law fit.

other long-range forces, such as Van der Waals forces. In addition, this method is extremely sensitive to minute amounts of charge, since relative changes in the cantilever resonance frequency $\Delta\nu/\nu \sim 3 \times 10^{-6}$ can be routinely measured.

Absolute magnitudes for the dielectric constant and surface charge can be obtained by fitting the EFM signal. However, these values depend strongly on the capacitance of the tip-substrate system. This capacitance is extremely sensitive to geometric details, thus making calculations unreliable. Instead, the tip-substrate capacitance can be measured directly, as shown in Fig. 2. An analytic expression is fit to d^2C/dz^2 as a function of z , and the resulting expression is then integrated twice to obtain the capacitance. From the theoretical fits, the capacitance is found to have a power law dependence given by $C(z) \sim z^{-1.2}$. This implies that the tip-substrate capacitance lies between a sphere-plane ($C \sim z^{-2}$) and a cone-plane ($C \sim z^{-1}$) geometry [22]. Since an AFM tip has square-pyramidal geometry, this seems quite reasonable.

From the above expressions, the change in $\Delta\nu(\omega)$ and $\Delta\nu(2\omega)$ as the AFM tip passes over a CdSe nanocrystal can be calculated. The component of the electrostatic force gradient at 2ω is sensitive to dielectric properties of the sample. Therefore, an increase in the magnitude of the resonance frequency when over a nanocrystal is expected due to the larger dielectric constant of CdSe compared with the surrounding air. For the component of the force gradient at ω , there are three possible types of behavior. When over a nanocrystal, a decrease (or increase) in cantilever resonant frequency corresponds to, respectively, a positively (or negatively) charged nanocrystal. No observed change in the resonant frequency corresponds to a neutral nanocrystal.

3.2. Properties of CdSe nanocrystals

Colloidal CdSe nanocrystals are synthesized using an organometallic synthesis developed in Ref. [23]. In this procedure, the nanocrystal size is controlled by adjusting the particle growth time in a hot, organic solvent. The solvent, trioctylphosphine oxide (TOPO), also acts to passivate the surface. The nanocrystal size (4.5 nm) is commonly determined from images taken with an AFM [21], and by comparing the measured absorption spectrum with spectra from nanocrystals with a known diameter [23]. A typical EFM sample consists of CdSe nanocrystals spun coat onto a thin 1–2 nm thick insulator layer, which is deposited on a metal substrate.

3.3. Electronic properties of CdSe nanocrystals

EFM images are recorded in dry air at room temperature, in a two-pass configuration [21]. First, a line scan of the sample topography is obtained. Second, the cantilever is raised a defined distance and scanned straight across at a constant height above the substrate. It is during the second line scan that the EFM signal is recorded. The components of the electrostatic force gradient at ω and 2ω , (the charge and dielectric image), are acquired simultaneously. A typical set of EFM images for individual CdSe nanocrystals is shown in Fig. 3 [21]. As shown in Fig. 3(c), the 2ω component of the electrostatic force gradient acting on the AFM tip is essentially uniform for all nanocrystals. However, the ω component of the electrostatic force gradient is highly non-uniform from nanocrystal to nanocrystal (Fig. 3(b)). Approximately half of the nanocrystals have a positive electrostatic force gradient, corresponding to a positive polarization. The other half have no detectable signals, and thus is nominally neutral, as expected for a dielectric particle with no additional charge carriers.

From absolute measurements of $\Delta\nu(2\omega)$, the magnitude of the static dielectric constant for a single CdSe nanocrystal is determined to be $\epsilon_0 \sim 8 \pm 3$. Within experimental uncertainty this value agrees with the value of the static dielectric constant in bulk CdSe, $\epsilon_0 \sim 9.5$ [24]. Future measurements can reduce the uncertainty in ϵ_0 by simultaneously measuring CdSe nanocrystals, and a material with a known dielectric constant. This can be accomplished, for example, with EFM measurements of CdSe and metal nanocrystals with the same diameter. Assuming the metal nanocrystals have an infinite static dielectric constant, a simple, relative comparison of $\Delta\nu(2\omega)$ between CdSe and the metal directly results in an accurate measure of ϵ_0 .

From theoretical modeling of $\Delta\nu(\omega)$, the magnitude of the electrostatic polarization for individual nanocrystals can be evaluated. However, given the current dynamic range of EFM measurements, the origin of the observed electrostatic polarization cannot be uniquely

determined. If the entire electrostatic polarization arises due to monopole terms, half of the nanocrystals have a screened, partial positive charge of $Q \sim 0.5 e$. If instead

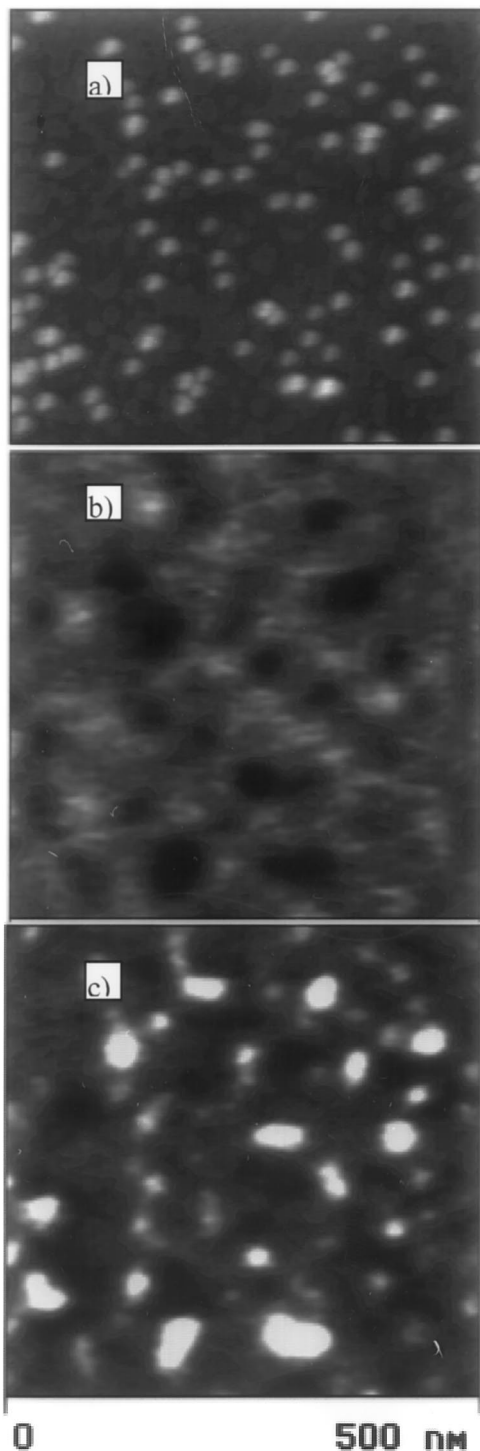


Fig. 3. EFM image of CdSe nanocrystals adapted from Ref. [21]. The substrate is poly(vinyl-butryal) spun coat on highly oriented pyrolytic graphite (a) tapping mode AFM height image. The scale in the vertical direction is 10 nm. The images in (b) and (c) correspond to the change in cantilever resonant frequency, $\Delta\nu$, at ω and 2ω , respectively.

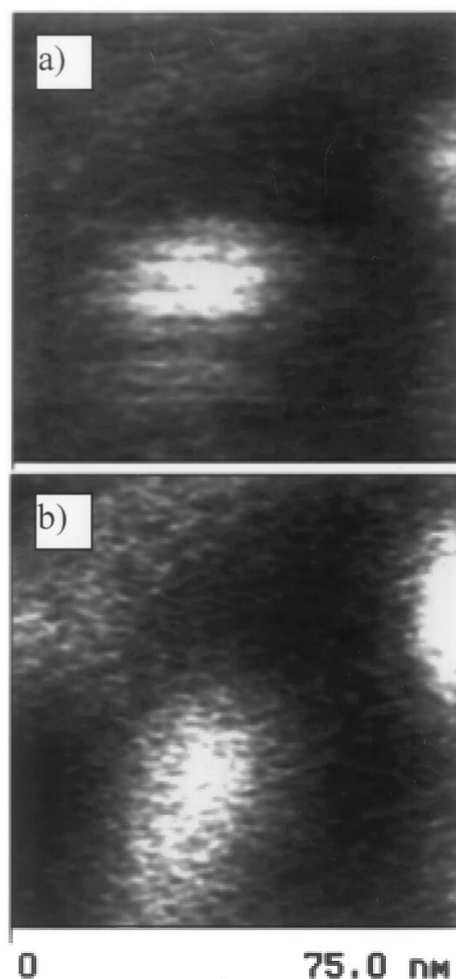


Fig. 4. (a) Charge (ω) and (b) dielectric (2ω) EFM image showing a blinking behavior in the polarization of an individual CdSe nanocrystal. The slightly elliptical shape of the nanocrystal is due to piezoelectric scanner drift during the acquisition of the image.

dipole terms cause the observed polarization, (and the dipole points straight up towards the tip), the nanocrystals have a dipole strength of $P \sim 35 D$. This dipole can be either structural, or caused by a physical separation of the electron and hole wavefunctions inside the nanocrystal. It is also possible that both monopole and dipole terms contribute to the observed polarization. From the RMS noise in $\Delta\nu(\omega)$, half of the nanocrystals which appear ‘neutral’ must contain less than one-tenth of an elementary charge.

Occasionally, the positive polarization of a small fraction of nanocrystals exhibits a blinking, or intermittent behavior, as shown in Fig. 4 [21]. The positive polarization present in the upper portion of the image in Fig. 4(a), vanishes during the lower portion of the scan. No change occurs in the dielectric image (Fig. 4(b)). The timescale for the on–off behavior ranges from seconds to minutes. In addition, the magnitude of the polarization from one on period to another on period is the same.

Currently, the origins of the polarization of individual CdSe nanocrystals, and the on/off behavior of this polarization, are not understood. However, a positive polarization has been consistently observed in CdSe nanocrystals under a variety of imaging conditions, and for a variety of samples [21]. Thus, it is likely that the polarization of individual CdSe nanocrystals is a result of the preparation procedure. Regardless of the cause of the observed polarization, it is clear from these recent EFM measurements that a significant fraction of CdSe nanocrystals has internal electric fields. Thus,

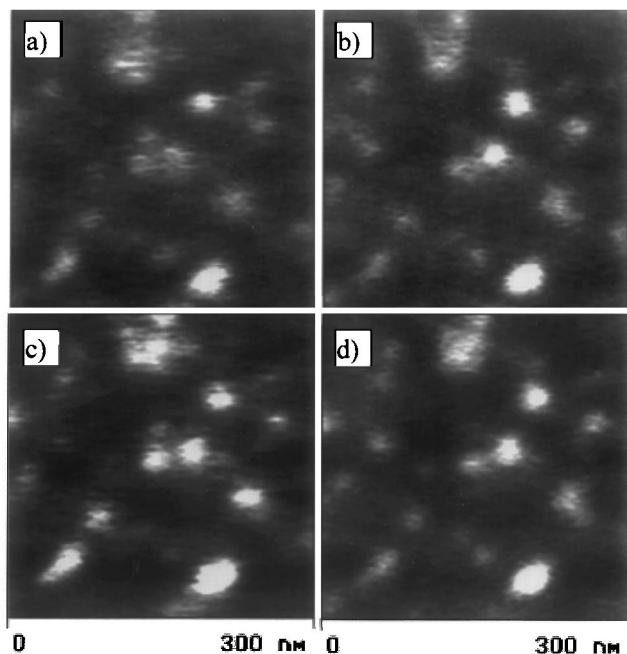


Fig. 5. Charge image before (a) and during (c) excitation at 442 nm. The corresponding dielectric image before (b) and during (d) photoexcitation. The laser power was $\sim 10 \text{ kW cm}^{-2}$ at the sample.

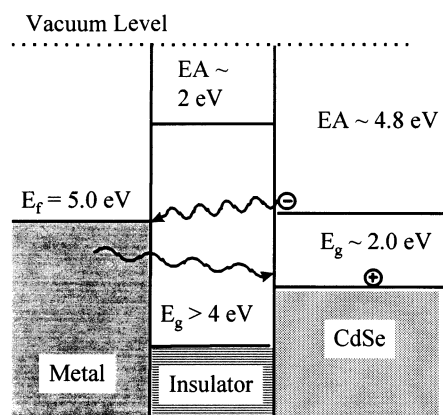


Fig. 6. Energy level diagram of a 5-nm diameter CdSe nanocrystal/insulator/metal junction. The electron affinity and ionization energy of the nanocrystal are estimated from bulk values [30] accounting for quantum confinement [31]. The Fermi energy for the metal is taken from the literature [32]. The values for the insulator are representative of typical values for similar organic materials.

current models used to explain a wide range of nanocrystal behavior, which implicitly assume an unpolarized nanocrystal, need to be questioned.

3.4. Photoionization of CdSe nanocrystals

EFM images are also obtained with simultaneous photoexcitation of CdSe nanocrystals, as shown in Fig. 5. Photoexcitation with energy greater than the nanocrystal band gap leads to an increase in the magnitude of positive charge on the nanocrystal by a factor of two [21]. Some nanocrystals, which were previously neutral, acquired a positive charge upon photoexcitation with magnitude $Q \sim 0.5 e$. Also, photoexcitation increases the number of nanocrystals which show an electrostatic-polarization blinking. Illumination with energy less than the band gap does not change the charge of CdSe nanocrystals. Photoionization of an individual nanocrystal was not instantaneous, but rather stochastic, with a time constant of minutes [21]. This photoinduced positive charge decayed back to the unexcited value with a much longer time constant of hours.

One mechanism consistent with photoionization of an individual nanocrystal involves tunneling of the excited electron into the metal substrate through the insulator layer [21]. This is represented graphically in Fig. 6. An electron is created in the nanocrystal, and primarily it recombines with the hole. However, a small, but finite, probability exists that the electron will tunnel into the metal through the insulator layer. The hole has an infinitesimally small probability of tunneling into the metal. This large asymmetry is due to the light electron effective mass ($m_e \sim 0.1 m_0$), the small band offset for electrons in the nanocrystal relative to the metal, and the large band offset for holes. When the exciting light is extinguished, the nanocrystal is therefore left with a positive charge. Eventually, an electron from the metal will tunnel back into the nanocrystal, recombine with the hole, and neutralize the photoinduced charge.

The fact that a photoexcited electron escapes the nanocrystal is not novel or entirely unexpected. In II–VI semiconductors, the hole has a large effective mass ($m_h \sim m_0$), while the electron is comparatively light. Therefore, in the nanocrystal the hole tends to be localized, while the electron is much more delocalized, with a non-negligible fraction of the electron density outside the nanocrystal [25]. Also, tunnel diodes made from CdSe nanocrystal monolayers, with an insulator layer thickness of 2–3 nm, were recently reported [26]. LEDs [27,28] and photovoltaic devices [29] based on electron transport through layers of CdSe nanocrystals have also been fabricated.

This elementary tunneling proposal for explaining the photoionization of individual nanocrystals must be

tested by further experiments. However, regardless of the underlying physical mechanism, it is clear that photoexcitation can lead to ionization of the nanocrystal. In addition, the photoinduced charge will entirely decay away over time. Furthermore, illumination results in a fraction of nanocrystals which subsequently show an on/off blinking of charge, with a timescale similar to that of single nanocrystal photoluminescence blinking. These observations provide direct evidence for the Auger photoionization mechanism [3] used to explain the blinking of single nanocrystal photoluminescence. With new commercial instrumentation combining optical and atomic force microscopy now available, in the near future, simultaneous measurements of single CdSe nanocrystal photoluminescence and photoionization can be attempted.

4. Future directions

Understanding the electronic properties of an individual semiconductor nanocrystal is an important issue not only at a fundamental level, but also with respect to the use of these materials for applications. However, our understanding is far from complete and it is clear that more work needs to be done in this area. Future work is likely to address the physical mechanisms responsible for the electrostatic polarization of individual nanocrystals both before and after photoexcitation. For example, the effects of surface passivation, and the degree of quantum confinement, on the electrostatic properties of a nanocrystal deserve study. Also, EFM measurements on non-spherical nanocrystals will determine size and shape effects on the polarization. Finally, the technique of EFM can be applied to study charge, and charge transport properties, in a wide array of self-assembled nanocrystal structures, ranging from nanocrystal devices, to nanocrystal solids.

Acknowledgements

The authors thank Zhonghua Yu and Guanglu Ge for assistance with nanocrystal synthesis and sample preparation, and Professor George Flynn for providing some equipment. We also acknowledge the support of the W.M. Keck foundation in the purchase of the AFM. This research was supported under NSF

MRSEC grant DMR-98-09687 for materials research at Columbia University.

References

- [1] A.D. Yoffe, *Adv. Phys.* 42 (1993) 173.
- [2] A.P. Alivisatos, *J. Phys. Chem.* 100 (1996) 13226.
- [3] M. Nirmal, B.O. Dabbousi, M.G. Bawendi, J.J. Macklin, J.K. Trautman, T.D. Harris, L.E. Brus, *Nature* 383 (1996) 802.
- [4] E. Rabani, B. Hetényi, B.J. Byrne, L.E. Brus, *J. Chem. Phys.* 110 (1999) 5355.
- [5] S.A. Blanton, R. Leheny, M.A. Hines, P. Guyot-Sionnest, *Phys. Rev. Lett.* 79 (1997) 865.
- [6] M.C. Klein, F. Hache, D. Ricard, C. Flytzanis, *Phys. Rev. B* 42 (1990) 11123.
- [7] M.E. Schmidt, S.A. Blanton, M.A. Hines, P. Guyot-Sionnest, *J. Chem. Phys.* 106 (1997) 5254.
- [8] J.J. Shiang, A.V. Kadavanich, R.K. Grubbs, A.P. Alivisatos, *J. Phys. Chem.* 99 (1995) 17417.
- [9] S.A. Empedocles, M.G. Bawendi, *Science* 278 (1997) 2114.
- [10] Al.L. Efros, A.L. Efros, *Sov. Phys. Semicond.* 16 (1982) 772.
- [11] E. Roca, C. Trallero-Giner, M. Cardona, *Phys. Rev. B* 49 (1994) 13704.
- [12] L. Brus, *Appl. Phys. A* 53 (1991) 465.
- [13] S.A. Empedocles, D.J. Norris, M.G. Bawendi, *Phys. Rev. Lett.* 77 (1996) 3873.
- [14] S. Empedocles, M. Bawendi, *Acc. Chem. Res.* 32 (1999) 389.
- [15] M. Nirmal, L. Brus, *Acc. Chem. Res.* 32 (1999) 407.
- [16] Al.L. Efros, M. Rosen, *Phys. Rev. Lett.* 78 (1997) 1110.
- [17] D.I. Chepic, Al.L. Efros, A.L. Ekimov, M.G. Ivanov, V.A. Karchenko, I.A. Kudriavtsev, T.V. Yazeva, *J. Lumin.* 47 (1990) 113.
- [18] Y. Martin, D.W. Abraham, H.K. Wickramasinghe, *Appl. Phys. Lett.* 52 (1988) 1103.
- [19] B.D. Terris, J.E. Stern, D. Rugar, H.J. Mamin, *Phys. Rev. Lett.* 63 (1989) 2669.
- [20] Y. Martin, C.C. Williams, H.K. Wickramasinghe, *J. Appl. Phys.* 61 (1987) 4723.
- [21] T.D. Krauss, L.E. Brus, *Phys. Rev. Lett.*, in press.
- [22] S. Belaidi, P. Girard, G. Leveque, *J. Appl. Phys.* 81 (1997) 1023.
- [23] C.B. Murray, D.J. Norris, M.G. Bawendi, *J. Am. Chem. Soc.* 115 (1993) 8706.
- [24] R. Geick, C.H. Perry, *J. Appl. Phys.* 37 (1966) 1994.
- [25] D. Schooss, A. Mews, A. Eychmüller, H. Weller, *Phys. Rev. B* 49 (1994) 17072.
- [26] S.-H. Kim, G. Markovich, S. Rezvani, S.H. Choi, K.L. Wang, J.R. Heath, *Appl. Phys. Lett.* 74 (1999) 317.
- [27] V.L. Colvin, M.C. Schlamp, A.P. Alivisatos, *Nature* 370 (1994) 354.
- [28] M.C. Schlamp, X. Peng, A.P. Alivisatos, *J. Appl. Phys.* 82 (1997) 5837.
- [29] N.C. Greenham, X. Peng, A.P. Alivisatos, *Phys. Rev. B* 54 (1996) 17628.
- [30] A.H. Nethercot, *Phys. Rev. Lett.* 33 (1974) 1088.
- [31] L.E. Brus, *J. Chem. Phys.* 79 (1983) 5566.
- [32] M. Böhmsch, F. Burmeister, A. Rettenberger, J. Zimmermann, J. Boneberg, P. Leiderer, *J. Phys. Chem. B* 101 (1997) 10162.